Systematic lipidomic analysis of yeast protein kinase and phosphatase mutants reveals novel insights into regulation of lipid homeostasis

Aline Xavier da Silveira dos Santos[a,b], Isabelle Riezman[a], Maria-Auxiliadora Aguilera-Romero[a,b], Fabrice David[c], Manuele Piccolis[d], Robbie Loewith[b,d], Olivier Schaad[a], and Howard Riezman[a,b]
[a]Department of Biochemistry, [b]National Centre of Competence in Research "Chemical Biology," and [d]Department of Molecular Biology, University of Geneva, Geneva CH-1211, Switzerland; [c]École Polytechnique Fédérale de Lausanne, Lausanne CH-1015, Switzerland

ABSTRACT **The regulatory pathways required to maintain eukaryotic lipid homeostasis are largely unknown. We developed a systematic approach to uncover new players in the regulation of lipid homeostasis. Through an unbiased mass spectrometry–based lipidomic screening, we quantified hundreds of lipid species, including glycerophospholipids, sphingolipids, and sterols, from a collection of 129 mutants in protein kinase and phosphatase genes of *Saccharomyces cerevisiae*. Our approach successfully identified known kinases involved in lipid homeostasis and uncovered new ones. By clustering analysis, we found connections between nutrient-sensing pathways and regulation of glycerophospholipids. Deletion of members of glucose- and nitrogen-sensing pathways showed reciprocal changes in glycerophospholipid acyl chain lengths. We also found several new candidates for the regulation of sphingolipid homeostasis, including a connection between inositol pyrophosphate metabolism and complex sphingolipid homeostasis through transcriptional regulation of *AUR1* and *SUR1*. This robust, systematic lipidomic approach constitutes a rich, new source of biological information and can be used to identify novel gene associations and function.**

Monitoring Editor
Sandra Lemmon
University of Miami

Received: Mar 31, 2014
Revised: Jul 8, 2014
Accepted: Aug 6, 2014

INTRODUCTION

Lipids are essential cellular constituents whose functions have been increasingly studied in recent decades. As a class of biomolecules, lipids present a vast diversity of structures (Brown and Murphy, 2009) and functions, with roles as building blocks of biological membranes, as well as in energy metabolism and signaling pathways (Dowhan, 1997; Leonard and Hurley, 2011). Lipids are essential components of all membranes in living organisms, and despite considerable differences in lipid composition of cells, organelles, and organisms, there is a high degree of conservation in the general framework of lipid metabolism and biological membrane properties throughout the kingdoms (Lykidis, 2007; Dennis *et al.*, 2010; Hannich *et al.*, 2011). In eukaryotic cells, the major membrane lipid components are glycerophospholipids, sphingolipids, and sterols (Daum *et al.*, 1998; Sampaio *et al.*, 2011). Among phospholipid and sphingolipid structures, there are many different combinations of fatty acids with different chain lengths, degrees of saturation, and head groups, giving rise to an extraordinary, although poorly understood, lipid complexity. The generation and maintenance of such diverse lipid compositions imply the existence of complex regulatory mechanisms (Dickson, 2008; Klose *et al.*, 2012; Zhang *et al.*, 2012).

Cells employ coordinated pathways of synthesis/degradation of phospholipids, sphingolipids, and sterols (Carman and Henry, 1999; Carman and Han, 2011; Nohturfft and Zhang, 2009; Gulati *et al.*, 2010; Rajakumari *et al.*, 2010; Gaspar *et al.*, 2011). These interconnected networks constitute a highly dynamic biological core that allows cells not only to adapt their lipid profile to environmental challenges, such as heat stress, osmotic stress, and nutrient

This article was published online ahead of print in MBoC in Press (http://www.molbiolcell.org/cgi/doi/10.1091/mbc.E14-03-0851) on August 20, 2014.
The authors declare no competing interests.
Address correspondence to: Howard Riezman (Howard.Riezman@unige.ch).
Abbreviations used: GC-MS, gas chromatography–mass spectrometry; IPC, inositol-phosphorylceramide; MIPC, mannose-inositol-phosphorylceramide; $M(IP)_2C$, mannose-(inositol-P)$_2$-ceramide; MRM-MS, multiple reaction-monitoring mass spectrometry; PC, phosphatidylcholine; PE, phosphatidylethanolamine; PI, phosphatidylinositol; PS, phosphatidylserine.

availability (Alvarez-Vasquez *et al.*, 2007; Zaman *et al.*, 2008; Ejsing *et al.*, 2009; Guan *et al.*, 2009; Young *et al.*, 2010; Gaspar *et al.*, 2011; Klose *et al.*, 2012), but also to sense the levels of the different lipids and adjust their lipid composition to preserve cellular functions (Tuller *et al.*, 1999; Gaspar, 2006; Guan *et al.*, 2009; Young *et al.*, 2010; De Smet *et al.*, 2012). Punctual perturbations in steps of lipid metabolic pathways can be compensated by the interlinked pathways, preserving cell viability with no obvious physiological consequences. Nevertheless, many important diseases have a lipid component in their epidemiology, highlighting the physiological consequences of an altered lipid homeostasis. Despite the obvious importance, relatively little is known about the regulatory mechanisms controlling lipid homeostasis (Holland and Summers, 2008; Petranovic *et al.*, 2010; Roelants *et al.*, 2010; Summers, 2010; Fu *et al.*, 2011).

With a few hundred lipid species and conserved lipid metabolic pathways with mammals, the yeast *Saccharomyces cerevisiae* represents a useful model organism for studying lipid homeostasis (Daum *et al.*, 1998; Ejsing *et al.*, 2009; Nielsen, 2009; Breslow and Weissman, 2010; Carman and Han, 2011; Santos and Riezman, 2012).

Protein phosphorylation is a major regulatory mechanism that controls many basic cellular processes in cells (Manning *et al.*, 2002; Tan *et al.*, 2009; Tan, 2011). A number of large-scale studies have been performed in *S. cerevisiae* to gather data and insights into phosphorylation-based signaling (Ptacek *et al.*, 2005; Fiedler *et al.*, 2009; Bodenmiller *et al.*, 2010; Breitkreutz *et al.*, 2010). Some key enzymes of lipid metabolism, including CTP synthase, PS synthase, choline kinase, and ORM proteins, have been already described as being regulated by phosphorylation (Kobayashi and Nagiec, 2003; Carman and Kersting, 2004; Choi *et al.*, 2010; Roelants *et al.*, 2010). However, until now, a systematic analysis of the effect of kinases and phosphatases on the lipid composition of a cell has not been done.

In this work, we analyzed the lipid composition of 129 yeast strains with gene deletions of nonessential kinases or phosphatases in a systematic approach to uncover new players in the regulation of lipid homeostasis.

RESULTS AND DISCUSSION

The large-scale lipidomic strategy

To assess the effect of a missing kinase or phosphatase on the lipid profile of *S. cerevisiae*, we systematically analyzed the lipidome of knockout strains of nonessential kinases and phosphatases (Supplemental Table S1). Strains were grown in rich media and harvested at early exponential growth phase. Using class-specific lipid extractions followed by mass spectrometry, our lipidomic approach covered most of the major lipid classes in yeast (Figure 1; Ejsing *et al.*, 2009; Guan *et al.*, 2010). For phospholipid and sphingolipid analysis, we used multiple-reaction monitoring mass spectrometry (MRM-MS), which allows a robust analysis of lipids of interest with high selectivity and sensitivity (Guan *et al.*, 2010). We monitored the signals of hundreds of lipid species (Supplemental Table S2), whose relative quantification was achieved using appropriate internal standards that were spiked into the sample before lipid extraction. For sterols, we used gas chromatography coupled to mass spectrometry (GC-MS). Ergosterol was identified by its pertinent fragment ions and retention time (Guan *et al.*, 2010).

We analyzed the lipid profile of 129 yeast knockout strains and wild type in biological duplicates with up to six technical replicates per biological replicate. To ensure consistent data quality for global comparison between the strains (i.e., to avoid biases arising from interplate variability), data were adjusted and normalized according to the batch of lipid extraction and analysis. We also applied filters

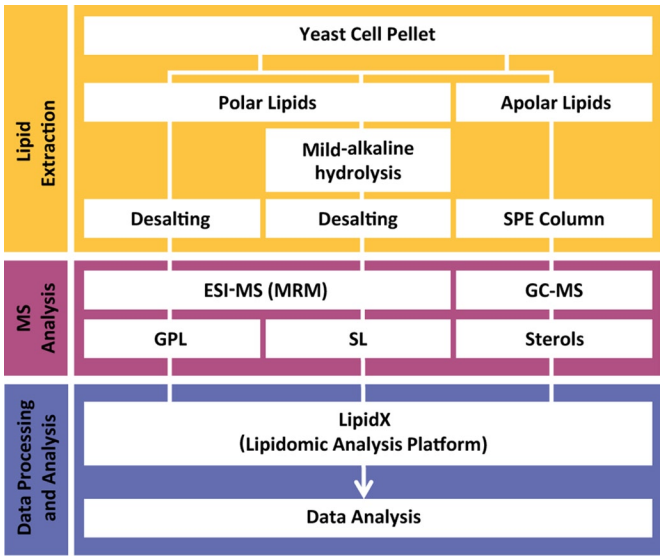

FIGURE 1: Workflow of lipid analysis. The lipid profile of yeast knockouts of protein kinase or phosphatase gene was systematically generated. Each strain was grown in standard conditions and processed in independent biological duplicates. Lipids were extracted according to different protocols and subjected to mass spectrometry analysis. Glycerophospholipids (GPLs) and sphingolipids (SLs) were analyzed by electrospray ionization mass spectrometry (ESI-MS) using multiple reaction monitoring. Sterols were analyzed using gas chromatography coupled to mass spectrometry (GC-MS). MS signal intensities were converted to relative concentrations based on standard curves of internal standards spiked in the samples before lipid extraction. Data were normalized and analyzed as described in *Materials and Methods* and the Supplemental Information.

based on 1) frequency of lipid detection along the screen and 2) average coefficient of variation of lipid detection between the biological replicates as a measure of quality control for lipid detection (Supplemental Information and Supplemental Figure S1). The final list of lipids contained 147 lipids whose acquisition was considered robust. Reproducibility of biological replicates was determined by coefficient of correlation, and highly disparate samples were removed from analysis. For lipid hit selection, we set fold-change thresholds combined with a moderate effect of strictly standardized mean difference (SSMD; Zhang, 2007; Zhang *et al.*, 2007; Supplemental Information and Supplemental Table S3).

We generated a comprehensive large-scale data set of lipid profiles with detailed features such as lipid class, chain length of the fatty acid moieties, unsaturation index, and number of hydroxylations. Our results provide data for lipids covering most of the major lipid classes in yeast in 127 mutant strains and wild types (Supplemental Table S4 and Supplemental Figure S3A). To ensure the specificity of our measurements, we selected representative samples from the screening for validation by high-resolution mass spectrometry using a Thermo Q Exactive mass spectrometer. The masses of the major lipids were detected with an average offset of <2 ppm, and the relative signal intensities of different lipids confirmed the results from the MRM screening (Supplemental Figure S2).

Our lipidomic approach is validated by comparison with data from the literature (described later). On the basis of the high-content data of this screening, we were able to perform multiple queries about patterns of lipid alterations that link kinases and phosphatases to the control of lipid homeostasis. Here we inspect the data for biological connections in the context of lipid homeostasis. In particular,

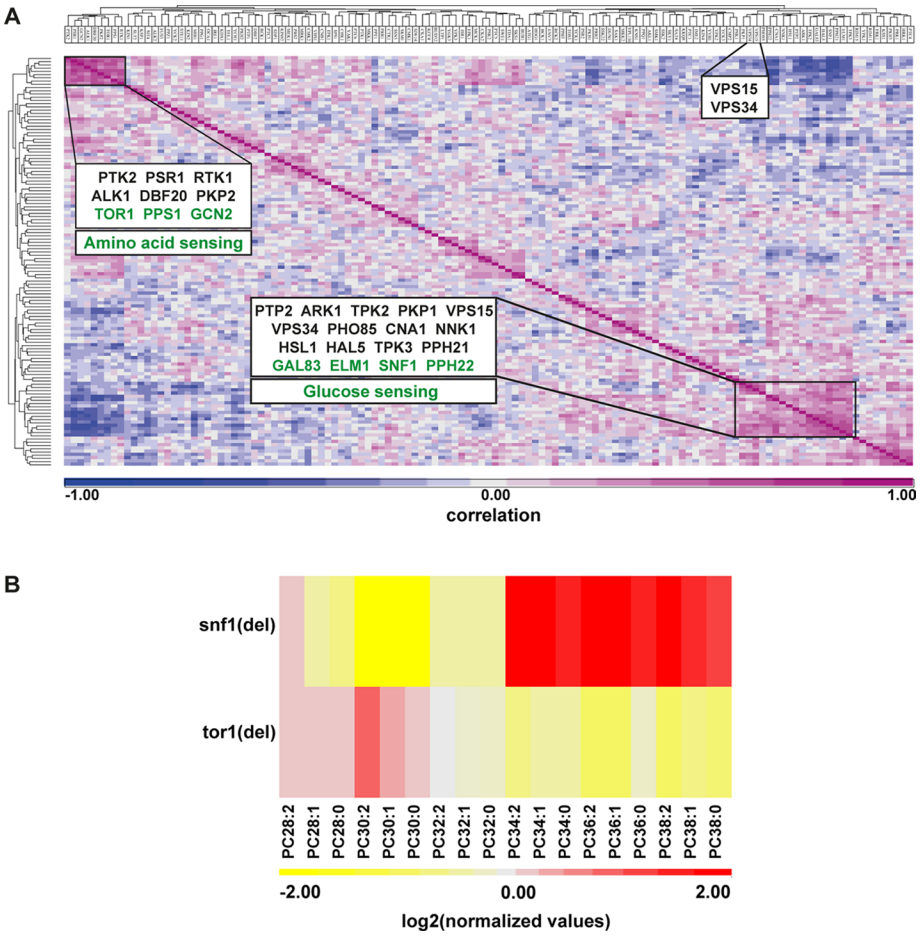

FIGURE 2: Overview of the screening: effect of kinase and phosphatase knockouts on the lipidome of yeast. (A) Correlation matrix of strains analyzed in the screening. Clusters of mutants involved in nutrient-sensing pathways are highlighted. Top right, *vps15*Δ and *vps34*Δ strains clustering together. (B) Strain-oriented query reveals detailed lipid profile of strains *snf1*Δ and *tor1*Δ, showing opposite lipid changes in PC species. Data given in Supplemental Tables S4 and S5.

we show that deletion of distinct members of signaling pathways involved in nutrient sensing have a large effect on the lipid profile. Through an unbiased approach, we found novel connections between nutrient-sensing pathways and the regulation of lipid metabolism (Kobayashi and Nagiec, 2003; Roelants *et al.*, 2011) and also uncovered new, unsuspected players in the regulation of lipid metabolism.

General aspects of lipid homeostasis revealed by large-scale screening

As a first unbiased attempt to find the similarities between lipid profiles of different mutants, we generated a correlation matrix of the mutants (Figure 2A). Two prominent clusters emerged, enriched in components of amino acid– and glucose-sensing pathways. By this exploratory approach, when one plots the quantities of all lipids relative to wild type for the 127 strains, high complexity is seen (Supplemental Figure S3A), suggesting that diverse signaling pathways control different aspects of lipid homeostasis. Of importance, using an unbiased clustering analysis, the *vps15* and *vps34* mutants clustered adjacent to each other. The two corresponding proteins are members of the same functional complex involved in autophagy and protein sorting (Obara *et al.*, 2008). This shows that our method of lipid profiling can give valuable information about biological function. This has important consequences because it suggests that determination of lipid profile is a useful tool to identify potential defects in cellular signaling pathways. Lipid alterations associated with disease could therefore be useful biomarkers to pinpoint disease mechanisms.

To simplify data analysis and uncover gene associations and regulatory pathways, we split the lipid data into major categories of interest. Lipids were classified according to their structural features into different lipid classes and subclasses based on their backbone, head group, fatty acid chain length, unsaturation index of the glycerophospholipids, and hydroxylation state of sphingolipids (Supplemental Table S2).

Concentrating on particular lipid classes, we were able to extract general information on the ability of yeast cells to remodel their lipid profile. Overall we noticed an interesting pattern in the magnitude of perturbations of each lipid class: the extent of changes (expressed as variance) of sphingolipids oscillated between 0.2 and 0.8, whereas that for total glycerophospholipids was between 0.05 and 0.08 (Supplemental Table S3 and Supplemental Figure S3B). These data suggest that the ceramide-sphingolipid pathway is more easily affected by disturbances in the kinase-phosphatase network compared with the glycerophospholipid pathway because they show a broader distribution in the magnitude of lipid amounts. Part of the explanation for this distinction could be the architecture of the biosynthesis and degradation pathways of these major groups: 1) ceramides and complex sphingolipids are synthesized in a linear manner with a single point of entry in the pathway through serine palmitoyltransferase with either conversion to complex sphingolipids or exit through a single portal (via the lyase, Dpl1p), whereas 2) phosphatidylcholine (PC), phosphatidylethanolamine (PE), phosphatidylinositol (PI), and phosphatidylserine (PS) have multiple paths of synthesis (de novo, Kennedy, and/or the reacylation of lysophospholipids; Supplemental Figure S4).

When comparing regulation of different lipid classes, we observed that PC and PE levels are highly correlated ($r = 0.71$; Supplemental Figure S5A). This suggests that the control of homeostasis of these two lipid classes is closely related and probably employs similar regulatory mechanisms. The ratio PE:PC in the plasma membrane has been proposed to be critical for plasma membrane stability, and mechanisms of control have been recently suggested (Roelants *et al.*, 2010; Tavassoli *et al.*, 2013). Pis1p and Cho1p compete for CDP-DAG for the synthesis of PI and PS, respectively, making this branch an important point of regulation (Henry *et al.*, 2012). Investigation of the mutants with unbalanced PI/PS ratio (Supplemental Figure S5B) reveals novel candidates for the regulation of this switch.

Sterols were the least affected of the lipid classes, with hits in <10% of the mutants (Supplemental Table S4 and Supplemental Figure S3B). Ergosterol is a main component of the yeast plasma membrane (Zinser *et al.*, 1993), and, not surprisingly, most genes of its synthesis are essential for cell viability; nonessential gene

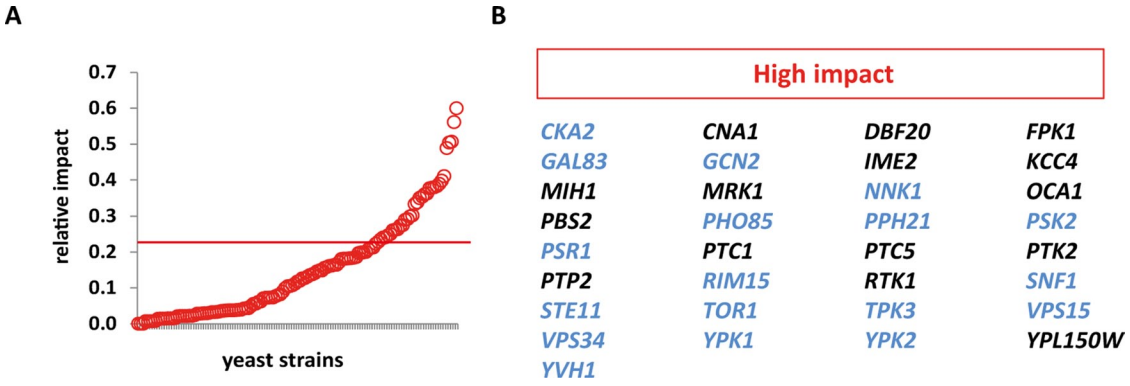

FIGURE 3: Nutrient-sensing pathways have a strong effect on the lipid profile. (A) The relative impact (RI) of a given knockout gene on the lipidome is a global measurement of disturbance in the lipid profile, calculated by the relative number of lipids that scored as a hit from all lipids analyzed (details in the text). High impact, RI > 0.22. (B) High-impact mutants implicated in nutrient-sensing pathways are highlighted in blue.

deletions cause many abnormalities (Munn *et al.*, 1999; Umebayashi and Nakano, 2003; Guan *et al.*, 2009; Aguilar *et al.*, 2010). Although regulation through gene expression is well described for ergosterol synthesis, enzymatic regulation of ergosterol biosynthesis steps is largely unknown, with no reference of phosphoregulation, suggesting that there might be minimal direct regulation (Sturley, 2000) by protein phosphorylation. Nevertheless, changes in sterol levels might arise by a secondary effect of changes in other lipid classes.

Global analysis reveals the effect of nutrient-sensing pathway on the lipidome

Given that kinases and phosphatases belong to highly interconnected networks (Sharifpoor *et al.*, 2012) with multiple compensatory effects, we anticipated that most of single-gene knockouts would have minimal consequences on the lipid profile. We decided to estimate the effect of a specific gene deletion on the lipidome as a function of the relative number of lipids that scored as a hit (Supplemental Information and Supplemental Table S6). Indeed, the majority of gene deletions had a minor effect on the lipidome (Figure 3A), and these small changes might simply reflect secondary effects. On the other hand, the high-impact group was enriched for members of central signaling pathways controlling metabolism. Kinases and phosphatases related to glucose metabolism (*SNF1*, *GAL83*, *PPH21*), nitrogen metabolism (*TOR1*, *GCN2*), phosphate metabolism (*PHO85*), and stress pathways (*PBS2*) were identified, suggesting that broad-spectrum signaling pathways might be important regulatory hubs of lipid homeostasis (Figure 3B).

The ability to adapt the membrane lipid profile to different environmental conditions seems to be an important adaptive feature of yeast. It was shown that the carbon source influences the glycerophospholipid and sphingolipid profile of yeast (Tuller *et al.*, 1999; Klose *et al.*, 2012). Nutrient-sensing mechanisms trigger multiple signaling pathways, which are finely orchestrated (Zaman *et al.*, 2008), but the functional wiring that connects nutrient sensing to lipid homeostasis is largely unknown. Our data reveal important candidates for these regulatory networks.

Glycerophospholipid homeostasis is linked to nutrient-sensing pathways

In *S. cerevisiae*, the major glycerophospholipids are PC, PE, PI, PS, phosphatidylglycerol, and cardiolipins. The control of glycerophospholipid homeostasis is fairly complex, with routes of synthesis, degradation, and recycling contributing to the overall lipid profile of a cell. The regulatory modes involve genetic and biochemical mechanisms (Henry *et al.*, 2012) in order to maintain a proper membrane lipid composition in response to changes in growth conditions.

Two important features of the lipidome with implications for membrane properties are the chain length and unsaturation index of fatty acids of glycerophospholipids. In *S. cerevisiae*, chain length is determined by the elongases Elo1p, Elo2p, and Elo3p, whereas desaturation is performed by Ole1p. Oleic acid (C18:1) and palmitoleic acid (C16:1) together with palmitic acid (C16:0) and stearic acid (C18:0), are the most abundant fatty acids in *S. cerevisiae* (Stukey *et al.*, 1989; Tehlivets *et al.*, 2007). The combination of fatty acids in the *sn-1* and *sn-2* positions of the glycerophosphate backbone differs in each lipid class (the major PC is PC32:2 and the major PE is 34:1; Supplemental Table S4), and the mechanism by which cells coordinate the different compositions is largely unknown (Boumann *et al.*, 2004b).

To address the mechanisms of control of these features through protein phosphorylation, we performed an unbiased comparison of lipidomics data from all the mutants. By hierarchical clustering based on the glycerophospholipid profiles, we observed two groups affecting the chain length of fatty acids with opposite effects. Among these, there were mutants in components of common signaling pathways—for example, in the glucose-sensing pathway, such as *SNF1*, *GAL83*, *ELM1*, *TOS3*, and *PPH21*—that caused an increase in the amounts of long-chain species of glycerophospholipids. In contrast, knockouts of *TOR1* and *GCN2* (among others) increased the amounts of short-chain-length species and decreased the levels of the longer ones (Supplemental Figure S6).

SNF1 and *TOR1* are major regulators of energy homeostasis in yeast. They are central players in glucose- and nitrogen-sensing pathways, respectively, as well as regulators of the switch between catabolism and anabolism. The signals triggered by Snf1p and Tor1p induce opposite responses (activation/repression) of similar processes (Usaite *et al.*, 2009; Zhang *et al.*, 2011). By comparing the changes in glycerophospholipid (GPL) profile in the two mutant strains (Figure 4A), we observed that the lipid composition also reflects this functional anticorrelation. The major differences between *snf1*Δ and *tor1*Δ mutants are in the fatty acid chain length of GPLs (Figure 2B and Supplemental Table S5).

Despite the clear lipid alterations promoted by the absence of nutrient-sensing pathway components, the mechanisms

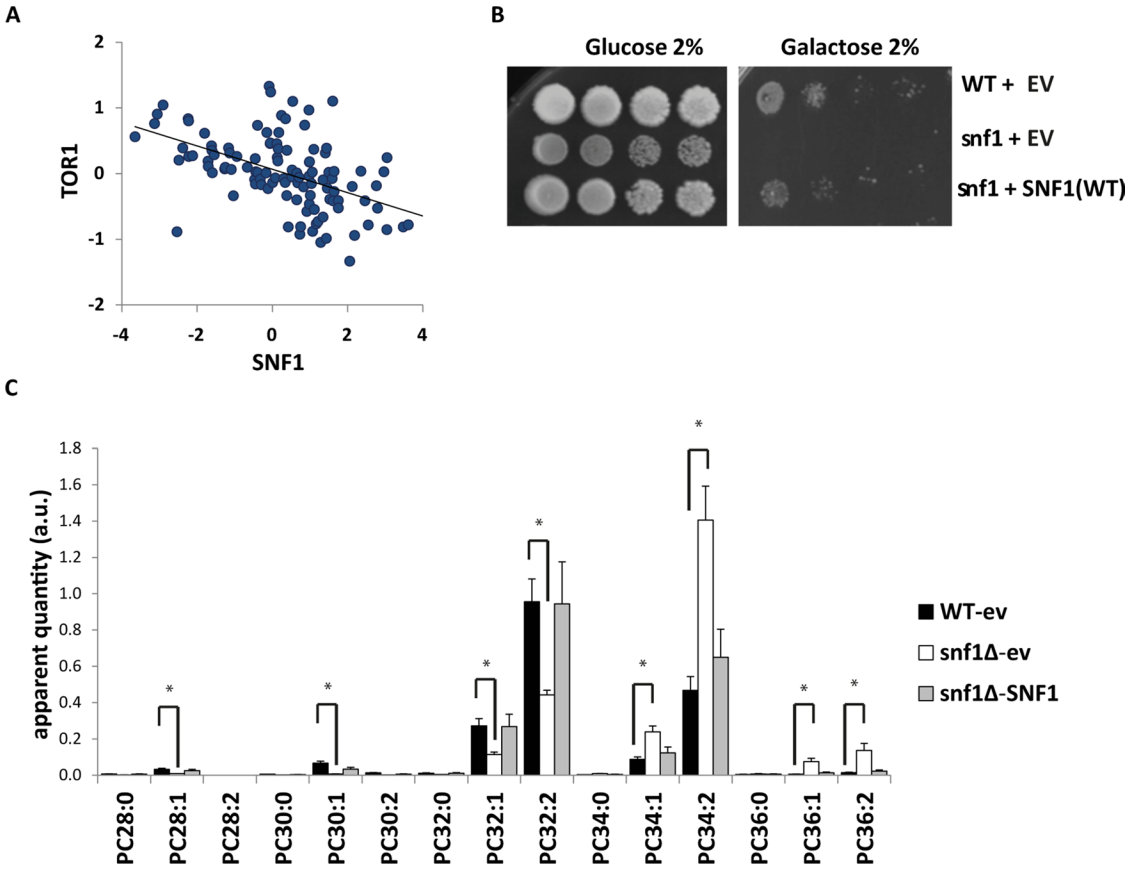

FIGURE 4: Nutrient-sensing pathways revealed by lipidomic screening. Global analysis of lipid changes revealed a strong effect of major nutrient-sensing pathways in the lipid profile of a cell. (A) Changes in glycerophospholipid profiles of *snf1*Δ and *tor1*Δ mutants are anticorrelated and reflect their opposite biological roles in cellular metabolism. (B, C) The *snf1*Δ mutant was complemented by *SNF1*, which also reversed its lipid profile back to wild-type cells. EV, empty vector. Data are median and SD of biological triplicates. *$p < 0.05$, *t* test.

behind this are not understood (Klose *et al.*, 2012). *SNF1* was first described as regulator of glucose repression (Celenza and Carlson, 1984), but its roles span the whole spectrum of cellular metabolism (Polge and Thomas, 2007; Usaite *et al.*, 2009). A defined linkage between *SNF1* and lipid metabolism occurs through the negative regulation of *ACC1* (acetyl-CoA carboxylase) upon glucose deprivation (Woods *et al.*, 1994). More recently, a lipid-related epistasis miniarray profile uncovered a negative genetic interaction of *SNF4* (a subunit of Snf1 kinase complex) with genes from the de novo biosynthesis of glycerophospholipids, suggesting that Snf1 signaling might coordinate the Kennedy pathway (Surma *et al.*, 2013).

We first confirmed the role of Snf1p in controlling the lipid profile by complementation of the *snf1*Δ strain with a plasmid carrying the *SNF1* gene (Figure 4B). The changes observed in the chain length of GPL in *snf1*Δ were reverted to wild-type levels by gene complementation (Figure 4C).

To obtain mechanistic insights, we then examined whether the changes in the lipid profile are related to preferential use of one of the two different biosynthetic routes for PC and PE (Henry *et al.*, 2012). GPLs of a mutant strain for the CDP-DAG pathway were reported to contain higher amounts of C18 than C16 fatty acyl chains (Schuiki *et al.*, 2010), which suggests that the glucose-sensing–related mutants might be using it preferentially, which would be consistent with negative regulation of the Kennedy pathway by Snf1p.

To test this hypothesis, we determined the lipid profile of *snf1*Δ cells in strains that possess only one functional biosynthetic route for PE and PC: either the CDP-DAG pathway (de novo; *cki1*Δ, *eki1*Δ, *dpl1*Δ, referred to as CEDΔ) or the Kennedy pathway (*psd1*Δ, *psd2*Δ, *ale1*Δ, referred to as PPAΔ; Figure 5A).

Analysis of the relative levels of GPL-containing short-chain (C28–C32) and long-chain (C34–C40) fatty acids showed that, in wild type (WT), there is a prevalence of long-chain fatty acids in PI, PS, and PE (and short chain in PC; Figure 5B, blue bars). This steady-state composition is a result of the contributions of both synthesis and turnover pathways. The lipid profile is altered when cells can use only the CDP-DAG pathway (CEDΔ), with the relative amount of short-chain fatty acids being higher (Figure 5B, red bars). In cells in which the CDP-DAG pathway was compromised and the GPLs were synthesized by the Kennedy pathway, the strain contained higher amounts of long-chain fatty acids, similar to the wild-type strain (Figure 5B, green bars). These results are consistent with previous reports of prevalence of C18 fatty acids via the Kennedy pathway (Schuiki *et al.*, 2010). At first surprising, the ratio between long and short PC species is somewhat less affected by the availability of a given biosynthetic route, as seen by the similar values for WT and mutant strains. However, the robustness of the PC profile is most likely due to both the use of the methylation pathway from PE to PC, which preferentially uses the short species PE32:2 as a substrate (Boumann *et al.*, 2004a), and the constant remodeling of newly

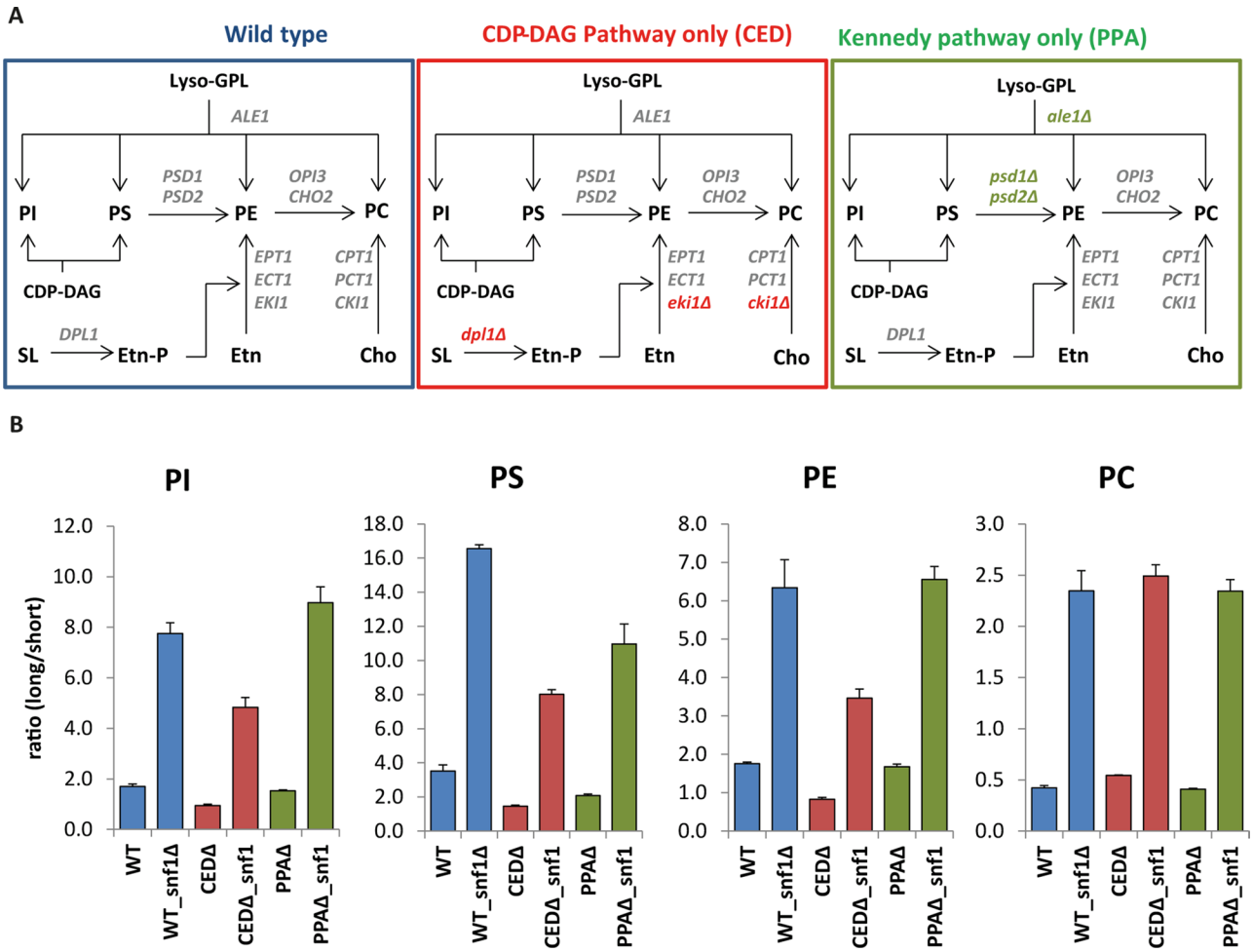

FIGURE 5: *SNF1* regulates the homeostasis of fatty acid chain length in glycerophospholipids. (A) Scheme of GPL biosynthesis in *S. cerevisiae*. Under normal conditions, the CDP-DAG pathway (red box) is the major route for synthesis of GPLs with a contribution of the Kennedy pathway (green box). (B) Ratio of long-chain fatty acids (FAs; >C18) over short-chain FAs (<C16) in GPL. WT strain (blue bars) and a strain containing only the Kennedy pathway (*PPA*Δ, green bars) have a prevalence of long-chain FAs in PI, PS, and PE but not in PC. The strain containing only CDP-DAG pathway (*CED*Δ, red bars) has similar amounts of long- and short- chain FAs in PI, PS, and PE and a prevalence of short-chain FAs in PC. *SNF1* deletion caused a general increase in the amount of long-chain FAs in all GPLs. No selective effect of *SNF1* deletion on the CDP-DAG or Kennedy pathway was observed. Data are represented as ratio of long/short GPLs. Mean and SD of three independent biological replicates are shown. Data given in Supplemental Table S11.

synthesized PC species (Boumann *et al.*, 2003). Moreover, a functional Kennedy pathway has been described as required for maintenance of the steady-state PC profile, specifically for the incorporation of C16:0 acyl chains (de Kroon, 2007; De Smet *et al.*, 2012), which is in agreement with the observed decrease in PC32:1 but not PC32:2 in CED cells (Supplemental Table S11).

When *SNF1* was disrupted, we observed a general increase in the levels of GPLs with long-chain fatty acids in all lipid classes. Of importance, this effect was not pathway dependent. On *SNF1* deletion, both mutant strains showed a substantial increase of long-chain-containing GPL as compared with the reference strains (Figure 5).

Therefore this experiment confirmed that the CDP-DAG and Kennedy pathways generate different lipid species of PE and PC, which reflects the previously suggested different fatty acid selectivity between the two pathways. It also showed that the effect of *SNF1* deletion on length of fatty acyl chains and the steady-state levels of GPL is independent of the synthetic pathway being used (CDP-DAG or Kennedy pathway).

Instead of pathway substrate selectivity, our data suggest that deletion of *SNF1* causes an increase in the availability of long-chain fatty acids, which would be incorporated by both synthesizing pathways. Given that Snf1p is a negative regulator of Acc1p, one can envisage a scenario in which, upon *SNF1* deletion, Acc1p activity is higher, increasing the levels of malonyl CoA (Shirra *et al.*, 2001; Shin *et al.*, 2012), a substrate for fatty acid elongation by the elongases Elo1 and Elo2p (Tehlivets *et al.*, 2007). The greater abundance of long-chain fatty acids would then be reflected in an unbalanced ratio of long- and short-chain fatty acids.

Our data not only imply that the glucose signaling pathway is linked to the GPL profile via regulation of fatty acid metabolism, they also suggest that Snf1p plays a biological role under nutrient-rich conditions (>1.5% glucose), in which it is allegedly inactive (Momcilovic and Carlson, 2011).

Curiously, data from a phosphoproteomic study (Bodenmiller *et al.*, 2010) revealed that the Pct1p phosphorylation (choline-phosphate cytidyltransferase, a rate-determining enzyme of the

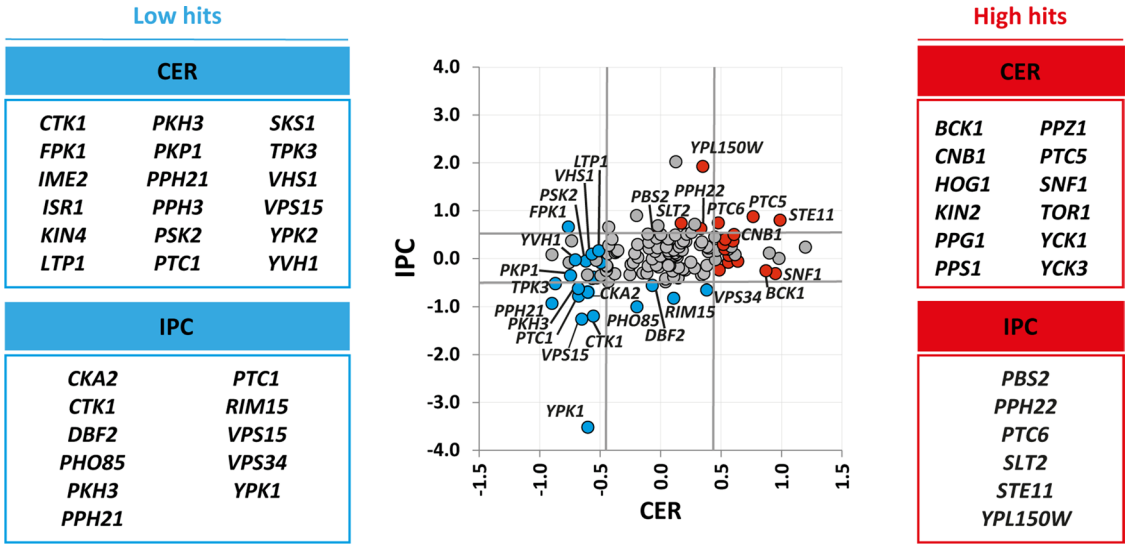

FIGURE 6: Novel candidates for regulation of sphingolipid homeostasis. (A) Relative changes (log_2[normalized data]) in total amounts of ceramides (CER) and the major complex sphingolipid (IPC). Strains that scored as a hit for low levels (blue) or high levels (red) are listed. Details are in the text.

CDP-choline branch of the Kennedy pathway) is strongly reduced in *snf1*Δ, which suggests a certain level of regulation of the pathway (which might be masked by the overall effect of high levels of long-chain fatty acids in our measurements).

Among the mutants with a large effect on GPL, *vps15*Δ and *vps34*Δ mutants shared some of the lipid phenotypes with *snf1*Δ. *VPS15* and *VPS34* are genes that code for the protein complex responsible for phosphatidylinositol 3-phosphate synthesis (Strahl and Thorner, 2007). Although initially puzzling, a biological connection has recently been described showing that that the mammalian homologue of Snf1p, AMP kinase, controls the activity of Vps34p complexes in mammalian cells during nutrient stress and autophagy (Kim *et al.*, 2013). Our data suggest that this new biological connection might be conserved from yeast to mammals, opening up the possibility of using yeast genetics to understand the mechanism. Consistent with a fairly direct connection of nutrient sensing and lipid homeostasis, *vps15*Δ and *vps34*Δ mutants also affect the phosphorylation of the same Pct1p phosphopeptide (Bodenmiller *et al.*, 2010).

Revealing new candidates of sphingolipid homeostasis

Despite the significance of sphingolipid intermediates as bioactive molecules involved in key physiological and pathological processes, we are just starting to understand the control of their homeostasis (Cowart and Hannun, 2007; Brice *et al.*, 2009; Roelants *et al.*, 2011; Liu *et al.*, 2012). In our search for novel regulators of the sphingolipid pathway, we sought concurrent changes in the levels of ceramides and complex sphingolipids as a indicator of the pathway activity. Ceramides and inositolphosphorylceramide (IPC), which is a major subclass of complex sphingolipids, were quantified. We found a number of candidates with alterations in these lipid classes, and, as expected, our lipidomic analysis revealed *cka2*Δ and *ypk1*Δ as strong positive regulators of sphingolipid amounts (Figure 6). Indeed, they regulate ceramide synthase (Kobayashi and Nagiec, 2003) and Orm proteins (Roelants *et al.*, 2011; Sun *et al.*, 2012), respectively. We also found increased amounts of sphingolipids in *tor1*Δ, which is in agreement with the recent finding of its role in the negative regulation of Orm proteins (Shimobayashi *et al.*, 2013).

Among the other strains with low levels of ceramides and IPC, one unsuspected mutant is *ctk1*Δ. *CTK1* is a subunit of C-terminal domain kinase (CTDK-1) that is involved in transcriptional regulation and translational events (Hampsey and Kinzy, 2007). Of interest, data from a phosphoproteomic study (Bodenmiller *et al.*, 2010) showed that Ypk1p phosphorylation is strongly reduced in *ctk1*Δ, which was confirmed here (Supplemental Figure S7A). Analysis of the same phosphoproteomic data also showed that *YPK1* and *CTK1* share multiple coregulated phosphopeptides, reinforcing the idea that they work on similar pathways (Supplemental Figure S7B). This scenario suggests that *CTK1* is a novel regulator of sphingolipid homeostasis, but the mechanisms remain to be elucidated.

In the groups of mutants with increased amounts of ceramides and sphingolipids, we noticed the presence of mutants involved in the osmotic response pathway, such as *hog1*Δ, *slt2*Δ, and *pbs2*Δ (Figure 6). Alterations in the availability of free water and osmotic pressure regulation are two of the most basic challenges of living cells, and, not surprisingly, osmoadaptation mechanisms are essential and well-conserved cellular features (Hohmann, 2002). A high-osmolarity shock triggers the high-osmolarity (HOG) pathway, whereas a low-osmolarity shock activates a cell wall integrity pathway (Supplemental Figure S8), both of which ultimately orient cells to adjust their metabolism and surface properties (Hohmann, 2002). Several mutants of the high-osmolarity and cell wall integrity pathways were found to be sensitive to inhibitors of sphingolipid synthesis, aureobasidin and/or myriocin (Hillenmeyer *et al.*, 2008). Inhibition of sphingolipid synthesis has also been reported to activate protein kinase C signaling (Jesch *et al.*, 2010).

It was reported that inhibition of sphingolipid synthesis results in activation of the HOG pathway (Barbosa *et al.*, 2011; Tanigawa *et al.*, 2012). Our results suggest a feedback between osmotic stress signals and sphingolipid homeostasis. Previous work showed a link between membrane tension and control of sphingolipid metabolism through relocalization of Slm1p to activate TOR complex 2 (Berchtold *et al.*, 2012). In this model, membrane stretching activates Slm1 protein relocalization, and reducing the osmolarity of the medium induces Slm protein relocalization through changes in membrane tension (Berchtold *et al.*, 2012). Our results suggest that an increase in osmolarity, detected through the HOG pathway,

works to oppose sphingolipid biosynthesis. We do not know whether the high-osmolarity response acts through Slm proteins and TOR complex 2.

In yeast, most of the C24-C26 fatty acids are found in sphingolipids, which are located primarily on the plasma membrane. Although sphingolipids are essential for cell viability, a mutant has been described that is able to survive in the absence of sphingolipids by producing compensatory glycerophospholipids containing a very long chain fatty acid (PI44:1 and PI42:1, not normally abundant in the cells; Vionnet *et al.*, 2010). It has been proposed that these unusual glycerophospholipids can partially mimic the structure and function of sphingolipids in the cellular membranes (Schneiter *et al.*, 2004). We observed that mutants with low levels of complex sphingolipids also show increased levels of C24- or C26-based PI (Supplemental Figure S9). One of those, *pho85*Δ, has a negative genetic interaction with *elo3*Δ (Huang *et al.*, 2002), which might arise due to defects in both sphingolipid regulation and compensatory pathways to produce C26-PI.

Our lipid analysis revealed that *pho85*Δ cells presented a unique sphingolipid profile (Figure 7A and Supplemental Table S5), leading us to hypothesize a link between sphingolipid metabolism and phosphate-sensing pathways. This mutant showed an accumulation of mannose-inositol-phosphorylceramide (MIPC) and reduced amounts of IPC. Results with mannose-(inositol-P)$_2$-ceramide (M(IP)$_2$C) in this mutant were not statistically significant and therefore are not discussed here. The Pho80-Pho85 cyclin/cyclin-dependent-kinase (CDK) complex is a key component of the phosphate (PHO) signaling response in yeast. Inositol-pyrophosphates are highly energetic molecules with functions in different cellular processes (Bennett *et al.*, 2006). They are formed by the sequential phosphorylation of inositol-triphosphate (IP$_3$) to IP$_4$ and IP$_5$ by Arg-82 and then to IP$_6$ by Ipk1p. In yeast, IP$_7$ can be synthesized by Vip1p (1PP-IP$_5$) or Kcs1p (5PP-IP$_5$), but only the product from Vip1p has been described as a specific inhibitor of the Pho80-Pho85 cyclin/CDK complex in a Pho81-dependent manner (Figure 7B; Lee *et al.*, 2007).

We determined the sphingolipid profiles of *vip1*Δ and *kcs1*Δ mutants, and results showed that *kcs1*Δ mutation produced a perturbation similar to *pho85*Δ, whereas the *vip1*Δ mutant was rather unaffected (Figure 7A and Supplemental Table S7). It has been described that the *kcs1*Δ mutant has an activated Pho4 pathway (Lee *et al.*, 2007). The Pho85-Pho80 CDK complex regulates the expression of genes involved in phosphate metabolism by controlling the phosphorylation state and localization of the transcription factor *PHO4*. Under phosphate-rich conditions, Pho4p is phosphorylated and localizes in the cytosol. However, under phosphate starvation, the CDK inhibitor Pho81p inactivates the complex, which ultimately causes accumulation of nonphosphorylated Pho4p in the nucleus, where it induces transcription of phosphate-responsive genes. The lipidomic results suggest that sphingolipid homeostasis is affected by a perturbed phosphate-sensing pathway. Of interest, it has been recently described that under low-P$_i$ conditions, Pho4p occupancy is highly enriched on the *SUR1* gene, which encodes for the catalytic subunit of MIPC synthase (Zhou and O'Shea, 2011). Thus we tested whether *SUR1* transcription was affected in the *pho85*Δ mutant, in which Pho4p is fully active (O'Neill *et al.*, 1996), and, as expected, *SUR1* mRNA expression was increased in *pho85*Δ cells (Figure 7C). We also measured the IPC synthase (*AUR1*) transcript levels and found reduced amounts in *pho85*Δ. These results are in agreement with the lipid profile of *pho85*Δ and thus suggest that sphingolipid homeostasis is regulated at the mRNA level by phosphate-sensing signaling pathways.

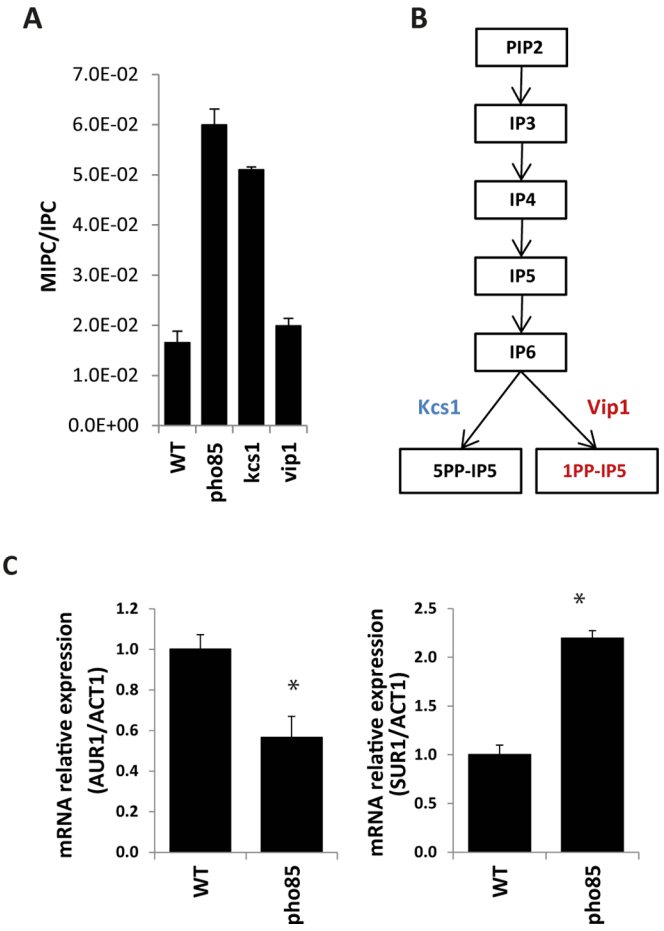

FIGURE 7: A connection between phosphate metabolism and sphingolipids. (A) Sphingolipid profile of *pho85*Δ, *kcs1*Δ, and *vip1*Δ mutants, showing an imbalance in MIPC/IPC levels in *pho85*Δ and *kcs1*Δ. Data for IPC-C 44:0 and MIPC-C 44:0 (from Supplemental Table S8). (B) The inositol pyrophosphate pathway. The 1PP-IP$_5$ (IP$_7$) produced by Vip1 acts as a cofactor of Pho81, an inhibitor of CDK. Inactive CDK results in accumulation of nonphosphorylated Pho4 (not shown) in the nucleus, where it activates gene transcription. (C) Relative amounts of mRNA expression of *AUR1* and *SUR1* genes from the sphingolipid biosynthesis pathway (see Figure 4). Data from three independent biological replicates. Mean and SD. *$p < 0.05$, *t* test.

Functional nonredundancy of homologous genes

In all organisms, a single-gene knockout frequently results in no obvious phenotype, which is often a consequence of redundancy between duplicated genes (Li *et al.*, 2010). Genetic redundancy not only provides robustness against deleterious mutations, but it is also a source of biochemical diversity, as the duplicated genes can accumulate mutations and eventually diverge functionally (Gu *et al.*, 2003). Many genes coding for protein kinases and phosphatases in *S. cerevisiae* have paralogues that arose from whole-genome duplication. One could expect that, due to compensation, single deletion of paralogous genes would have minimal effect on the lipidome and thus would be less frequent in the group of mutants with large effect on the lipidome. Yet we observed that 38% of the high-impact genes had a paralogue counterpart (Supplemental Table S8). Diversification of duplicated genes is commonly asymmetric, that is, one of the duplicates is often more expressed and has more molecular and genetic interactions than the other (Wagner, 2002).

Our results showed that when considering the lipid profile, genes whose deletion had a large effect on the lipidome often had a paralogue with negligible effect (Supplemental Tables S5 and S8).

Between *CNA1* and *CMP2* (which, together with *CNB1*, are the subunits of the calcineurin A complex), only deletion of *CNA1* had a strong effect, mostly observed as the reduction of lipids with short-chain fatty acids. Cna1p (but not Cmp2p) has been reported to interact with the long-chain fatty acyl-CoA synthetase (Faa4p), which is responsible for activation of exogenous long-chain fatty acids (Breitkreutz *et al.*, 2010), suggesting a distinct role for *CNA1* in lipid metabolism.

The glycogen synthase kinase (GSK-3) has four different isoforms in yeast (*MRK1*, *RIM11*, *YGK3*, and *MCK1*). *MRK1* and *RIM11* are paralogous genes with known divergent functions: *RIM11* is involved in meiosis (Bowdish *et al.*, 1994), whereas *MRK1* is important for growth at high temperature (Hirata *et al.*, 2003). Deletion of *MRK1* caused an increase in phospholipids with shorter chain length, suggesting that *MRK1* requirements for growth at high temperature could be related to the increase in chain length observed in cells grown at 37°C (Klose *et al.*, 2012).

FPK1 and its paralogous gene, *KIN82*, have been described as regulators of aminophospholipid flippases (Nakano *et al.*, 2008), which are also involved in sphingolipid (Roelants *et al.*, 2009) and sterol homeostasis (Muthusamy *et al.*, 2009). In both *fpk1*Δ and *kin82*Δ mutants, the levels of ceramides are reduced, whereas ergosterol levels are increased in *fpk1*Δ but reduced in *kin82*Δ.

Our data also showed paralogous genes with a minimal effect on the lipid profile of cells, such as *CMK1*/*CMK2* and *SAK1*/*TOS3*. There are no reported connections between the calmodulin-dependent protein kinases Cmk1p and Cmk2p and lipid homeostasis in yeast, whereas the mammalian homologue, CaMKIIp, has been proposed to mediate lipolysis in adipocytes (Rapold *et al.*, 2013). Sak1p and Tos3p are upstream kinases of Snf1p, which are activated by glucose-sensing mechanisms (Hedbacker and Carlson, 2008). We found that Snf1p is a major regulator of lipid homeostasis in yeast, and, of interest, deletion of its third upstream activating kinase, *ELM1*, gives a similar lipid phenotype as *snf1*Δ. This suggests that *ELM1* is not functionally redundant with *SAK1* and *TOS3* for lipid homeostasis. The lack of lipid phenotype of *SAK1* and *TOS3* could be due to a functional redundancy or a lack of involvement in lipid homeostasis, but additional experiments would be required to test these possibilities.

Limitations of the analysis

We show here that systematic lipidomics of yeast mutants is a powerful tool for uncovering new pathways of regulation of lipid homeostasis. This study, however, reveals only a snapshot of all possible cell growth contexts, and we believe many other associations of kinases and phosphatases with control of lipid homeostasis can be revealed under different growth conditions. Our findings should thus serve as starting point for researchers in the field to explore a broader range of biologically relevant contexts, such as different growth phases, nutrient-depleted media, and different osmotic and pH conditions. In addition, our type of analysis does not differentiate between direct and indirect effects of the mutations studied. As with any screen of this type using a deletion mutant collection, care should be taken when interpreting the results. As shown here as an example for the *snf1*Δ mutant, it is advisable to perform complementation studies or recreate mutants freshly and retest before making definitive conclusions.

One avenue to differentiate between direct and indirect effects would be to use analogue-sensitive alleles of the kinases (Bishop *et al.*, 2000) and determine a time course of events in the change of the lipid profile.

Despite having covered many of the major membrane lipids in yeast, our targeted lipidomics analysis was clearly not exhaustive. Other biologically relevant lipid species, such as phosphoinositides, phosphatidic acid, and triacylglycerides, have not been included due to the need of specific extraction and analytical methods that did not fit our large-scale lipidomics pipeline.

Final considerations and perspectives

We present here a new approach to gaining novel insights into the regulation of lipid homeostasis. By approaching the data from an oriented perspective, we can shortlist mutants and/or lipid phenotypes of interest and evaluate their correlation with a specific biological phenomenon, as done here for our search for new regulators of sphingolipid homeostasis. However, one can also approach it from a discovery perspective, in which lipid patterns emerge from global unbiased comparison, revealing unprecedented biological connections, such as between nutrient-sensing pathways and glycerophospholipid homeostasis.

The precise mechanism controlling the functional relationship between nutrient-sensing pathways and lipid homeostasis remains to be studied in detail, but it seems clear that there is a regulation by the glucose-sensing signaling pathway. Of importance, our analysis was performed with cells grown to early log phase in rich media, in which canonical nutrient-sensing signaling, such as the glucose- and phosphate-sensing pathways, are believed to be inactive. Nevertheless, we found significant alterations in the lipid profile, calling into question this assumption and suggesting that Snf1p activity is required for the correct regulation of glycerophospholipid homeostasis under these conditions.

The conditions we used in our work are frequently used in laboratory experiments, and therefore our data should be relevant for data mining when searching for links between lipid composition and mutant phenotypes. In another attempt to find new players in lipid homeostasis, a recent study described a high-throughput lipidomic platform to screen yeast libraries (Tarasov *et al.*, 2014). With an unconventional approach based on cell cultures grown on solid media and collected at stationary phase, the data generated will be difficult to compare with data from standard culture conditions due to the strong effect of growth phase and nutrient availability on the lipid profile of cells (Carman and Han, 2011; Klose *et al.*, 2012; Jewett *et al.*, 2013).

For future data mining and to provide a better link to studies of metabolism in general, we ensured that the lipids we present here are all now entered into the Chemical Entities of Biological Interest database, facilitating future bioinformatics approaches (Supplemental Table S10). We presented a robust strategy to systematically analyze the lipidome of yeast on a relatively large scale, and the data generated here represent a novel, rich set of information to understand lipid homeostasis and provide links between lipid levels and other phenotypes. New technical improvements will be necessary to make this methodology truly high throughput, especially concerning standardizing growth conditions for high throughput and the amount of time spent on MS analysis.

Our systematic lipidomic approach not only shows high agreement with preexisting results in the literature, but it also has predictive power, as it revealed intricate connections between the lipid profile of a cell, nutrient-sensing mechanisms, and environmental conditions. The signaling pathways seen here are fairly well conserved in mammalian cells, and it is likely that they will also be used there, perhaps linked to other nutrient controls, to regulate lipid

homeostasis. Results of a similar analysis using small interfering RNA–treated cells for the mammalian kinome will test this hypothesis.

The kinase-phosphatase network of a cell is composed of a multitude of interactions and extensive cross-talk (Breitkreutz *et al.*, 2010). Many homologues in the protein kinase and phosphatase families that have been described to be functionally redundant, primarily for cell viability, showed distinct lipid patterns, suggesting that individual paralogues play distinct roles in lipid metabolism.

The data provided here contains a wealth of information, which will be further inspected for more biological and mechanistic connections in the context of lipid homeostasis. Owing to the close interaction between lipid metabolism and other cellular processes, such as energy homeostasis, gene regulation, membrane trafficking, and protein metabolism, it is clear that data from lipidomics studies are essential to comprehend the system as a whole. Finally, knowing the regulatory networks of lipid homeostasis is critical to tackling how its deregulation contributes to diseases, such as metabolic syndrome, Alzheimer disease, and genetic disorders of lipid catabolism (Outeiro and Muchowski, 2004; Smolenska-Sym *et al.*, 2004; Cookson *et al.*, 2011; Kaur *et al.*, 2013).

MATERIALS AND METHODS

Media, strains, and plasmids

Strains used in this study are presented in Supplemental Table S1. Yeast precultures were grown in rich medium (yeast extract/peptone/dextrose [YPD]: 2% glucose [Merck, Darmstadt, Germany], 1% Bacto Peptone [Difco, Allschwil, Switzerland], 2% Bacto Yeast Extract [Difco], 10 mM 2-(*N*-morpholino)ethanesulfonic acid [Sigma-Aldrich, Steinheim, Germany], 40 mg/ml L-tryptophan [Fluka, Steinheim, Germany], uracil [Sigma-Aldrich], and adenine ([Sigma-Aldrich]) to saturation and diluted to 0.003 OD_{600} unit/ml, and cultures were grown to early exponential phase (1– 2 OD_{600} units/ml) in YPD at 30°C. Preliminary experiments using wild-type cell cultures showed that glucose levels remained well above 1% under these growth conditions. Metabolism was quenched by addition of trichloroacetic acid (TCA) to a final concentration of 5% (vol/vol) and cooling on ice. Pellets equivalent to 25 OD_{600} units were washed with cold 5% TCA and rinsed with distilled water. Cell pellets were frozen and kept at –80°C until lipid extraction. *SNF1* constructs were expressed from its native promoter on a centromeric plasmid, pCE108 (Momcilovic and Carlson, 2011). Plasmid SNF1-WT was obtained from the lab of Marian Carlson (Columbia University Medical School, New York, NY). The *snf1*Δ strain was constructed by one-step gene replacement using standard protocols.

Chemicals and lipid standards

We used 17:0/14:1 PC (LM1004), 17:0/14:1 PE (LM-1104), 17:0/14:1 PI (LM-1504), 17:0/14:1 PS (LM-1304), C17 ceramide (860517), and C8-glucosyl(β) ceramide (860540) as internal lipid standards, which were purchased from Avanti Polar Lipids (Alabaster, AL). Cholesterol was used as sterol standard and was purchased from Fluka. Pyridine (ReagentPlus) and methylamine solution (33% in absolute ethanol) were from Sigma-Aldrich. HPLC-grade chloroform was purchased from Acros (Geel, Belgium), and LC-MS–grade methanol and LC-MS–grade ammonium acetate were from Fluka. LC-MS–grade water was purchased from Fisher Scientific (Loughborough, United Kingdom).

Lipid extraction and analysis

Glycerophospholipids and sphingolipids. Lipids were extracted as previously described (Guan *et al.*, 2010) with minor modifications. Briefly, cells (25 OD_{600} units) were resuspended in 1.5 ml of extraction solvent (ethanol, water, diethyl ether, pyridine, and 4.2 N ammonium hydroxide [15:15:5:1:0.018, vol/vol]). A mixture of internal standards (7.5 nmol of 17:0/14:1 PC, 7.5 nmol of 17:0/14:1 PE, 6.0 nmol of 17:0/14:1 PI, 4.0 nmol of 17:0/14:1 PS, 1.2 nmol of C17:0-ceramide, and 2.0 nmol of C8-glucosylceramide) and 250 µl of glass beads was added, the sample was vortexed vigorously (multitube vortexer; Labtek International, Christchurch, New Zealand) at maximum speed for 5 min and incubated at 60°C for 20 min. Cell debris was pelleted by centrifugation at 1800 × *g* for 5 min, and the supernatant was collected. The extraction was repeated once, and the supernatants were combined and dried under a stream of nitrogen or under vacuum in a Centrivap (Labconco, Kansas City, MO). The sample was divided into two equal aliquots. One half was used for ceramide and sphingolipid analysis, in which we performed an extra step to deacylate glycerophospholipids using monomethylamine reagent (methanol, water, *n*-butanol, methylamine solution [4:3:1:5, vol/vol]; Cheng *et al.*, 2001) to reduce ion suppression due to glycerophospholipids in sphingolipid detection. For desalting, both lipid extracts were resuspended in 300 µl of water-saturated butanol and sonicated for 5 min. We added 150 µl of LC-MS–grade water, and samples were vortexed and centrifuged at 3200 × *g* for 10 min to induce phase separation. The upper phase was collected. Another 300 µl of water-saturated butanol was added to the lower phase, and the process was repeated twice. The combined upper phases were dried and kept at –80°C until analysis. For glycerophospholipid and sphingolipid analysis by electrospray ionization-MS/MS, lipid extracts were resuspended in 500 µl of chloroform:methanol (1:1, vol/vol) and diluted in chloroform:methanol:water (2:7:1, vol/vol/vol) and chloroform:methanol (1:2, vol/vol) containing 5 mM ammonium acetate for positive and negative mode, respectively. A Triversa Nanomate (Advion, Ithaca, NY) was used to infuse samples with a gas pressure of 30 psi and a spray voltage of 1.2 kV on a TSQ Vantage (ThermoFisher Scientific, Waltham, MA). The mass spectrometer was operated with a spray voltage of 3.5 kV in positive mode and 3 kV in negative mode. The capillary temperature was set to 190°C. MRM-MS was used to identify and quantify lipid species as previously described (Guan *et al.*, 2010). Data were converted and quantified relative to standard curves of internal standards that had been spiked in before extraction. Two independent biological replicates were analyzed, each of which comprised up to six technical replicates.

For glycerophospholipid and sphingolipid analysis by high-resolution mass spectrometry, we used a Q Exactive Hybrid Quadrupole-Orbitrap Mass Spectrometer (Thermo Scientific). Lipid extracts were dissolved in 500 µl of chloroform:methanol (1:1, vol/vol) and diluted two times in 5 mM ammonium acetate in chloroform:methanol:water (2:7:1, vol/vol/vol) for both positive- and negative-ion-mode mass analysis. Samples were analyzed by direct infusion. Positive-ion-mode analysis was performed using scan range m/z = 650–800 (for monitoring PC and PE) and 540–750, using lock mass 588.4471 (for ceramides). Negative-ion-mode analysis was performed using scan range m/z = 700–850 (for monitoring PI and PS) and 550–1150 (for complex sphingolipids). The acquisition was set to 100 scans. Spectra were acquired using mass resolution of 280,000 and automatic gain control at $3e^6$. Lipid species were identified according to their m/z, and their abundance was calculated by their signal intensities relative to internal standards (17:0/14:1 PC for PC and PE, 17:0/14:1 PI for PI, 17:0/14:1 for PS, C8-glucosylceramide for complex sphingolipids, and C17 ceramide for ceramides).

Sterols. Briefly, cells (25 OD_{600} units) were resuspended in 600 µl of water and 1500 µl of methanol. Cells were vigorously vortexed for

5 min, and 750 µl of chloroform was added. Samples were vortexed and centrifuged for 1 min at 100 × *g* to pellet the beads and cell debris. The supernatant was transferred to a clean tube. The beads were washed once with 600 µl of chloroform:methanol [1:2, vol/vol]), the supernatant was combined with the first one, and 400 µl of water was added to induce phase separation. Samples were centrifuged for 10 min at 3200 × *g*, the aqueous upper phase was discarded, and the lower, organic phase was transferred to a new tube and dried. Samples were then fractionated on a solid-phase extraction column. Briefly, a silica column (SiOH, 100 mg/1 ml, Chromabond; Macherey-Nagel, Switzerland) was preequilibrated with 2× 1 ml of chloroform. Sample was resuspended in 250 µl of chloroform, vortexed well, sonicated for 5 min, and loaded on the column. The sample was eluted by addition of 2× 650 µl of chloroform. The eluent, containing the sterols, was dried and flushed with a steam of nitrogen before storage to avoid oxidation. Extracts were analyzed by GC-MS as previously described (Guan *et al.*, 2010).

Phosphate measurement. The total lipid extract was resuspended in 500 µl of chloroform:methanol (1:1, vol/vol), and 50 µl was placed in 13-mm disposable Pyrex tubes. After solvent evaporation, 20 µl of water and 140 µl of perchloric acid (70%) were added to the tubes. Samples were heated for 1 h at 100°C in a fume hood. Tubes were allowed to cool for 5 min at room temperature. Next 800 µl of freshly prepared water:1.25% NH_4 molybdate:1.67% ascorbic acid (5:2:1, vol/vol) was added to the tubes, followed by 5 min of heating at 180°C. Tubes were cooled at room temperature, and 100 µl was used for measurement of absorbance at 820 nm. A standard curve was generated with 0–20 µl of 3 mM KH_2PO_4 standard solution and processed identically.

Real-time PCR analysis. Total RNA was extracted using the RNeasy Mini Kit (Qiagen, Hilden, Germany). cDNA was synthesized by reverse transcription using Superscript II (Invitrogen, Zug, Switzerland) in a reaction of 1 µg of RNA, 1 µl of dNTPs (10 mM each; Invitrogen), 2 µl of hexamer (120 ng/µl), 4 µl of reverse transcriptase buffer, 2 µl of dithiothreitol (0.1 M), 0.5 µl of RNasin (40 U/µl; Promega, Dübendorf, Switzerland), and 1 µl of Superscript II. The reaction was composed of cycles of 10 min at 25°C, 50 min at 42°C, and 15 min at 70°C. Quantitative real-time PCR was done on an iCycler (Bio-Rad, Hercules, CA) with PCR System iQ SybrGreen Supermix (Bio-Rad). The list of primers is given in Supplemental Table S9. The reaction was composed of an initial incubation of 94°C for 1 min, followed by 40 cycles of 10 s at 95°C and 30 s at 60°C. All results were analyzed by the $2^{-\Delta\Delta CT}$ method (Livak and Schmittgen, 2001), using *ACT1* as a housekeeping gene.

Statistical methods

A detailed description of the lipidomic data analysis is given in the Supplemental Information. Unless otherwise noted, pairwise statistical analysis was based Student's *t* test, with $\alpha = 0.05$.

Information about lipid compounds annotated in this study is available on www.lipidomes.org.

ACKNOWLEDGMENTS

We thank the members of Riezman lab and the Protein Core Facility of the École Polytechnique Fédérale de Lausanne for discussions and technical support during the project, Victor Nesatyy for support with mass spectrometric data acquisition, Markus Wenk and Xue Li Guan for discussions and advice, Yann Desfougères and Andreas Meyer for insights into *kcs1*Δ and *vip1*Δ, Bernd Bodenmiller and Ruedi Aebersold for sharing phosphoproteomics data, and Claudine Kraft and Matthias Peter for providing the kinase/phosphatase gene deletion collection. The mapping of the lipid species to the Chemical Entities of Biological Interest ontology and the necessary ontology development were performed by Lucila Aimo, Anne Niknejad, and Alan Bridge of the Swiss Institute of Bioinformatics, with assistance from Chemical Entities of Biological Interest curators. This mapping and ontology development work was supported by SystemsX.ch and the Swiss Institute of Bioinformatics. Service and educational activities at the Swiss Institute of Bioinformatics are supported by the Swiss Federal Government through the State Secretariat for Education, Research and Innovation. This work was supported by grants from SystemsX.ch (LipidX.ch) evaluated by the Swiss National Science Foundation, the Swiss National Science Foundation (H.R.), and the National Centre of Competence in Research "Chemical Biology."

REFERENCES

Aguilar PS, Heiman MG, Walther TC, Engel A, Schwudke D, Gushwa N, Kurzchalia T, Walter P (2010). Structure of sterol aliphatic chains affects yeast cell shape and cell fusion during mating. Proc Natl Acad Sci USA 107, 4170–4175.

Alvarez-Vasquez F, Sims KJ, Voit EO, Hannun YA (2007). Coordination of the dynamics of yeast sphingolipid metabolism during the diauxic shift. Theor Biol Med Model 4, 42.

Barbosa AD, Osório H, Sims KJ, Almeida T, Alves M, Bielawski J, Amorim MA, Moradas-Ferreira P, Hannun YA, Costa V (2011). Role for Sit4p-dependent mitochondrial dysfunction in mediating the shortened chronological lifespan and oxidative stress sensitivity of Isc1p-deficient cells. Mol Microbiol 81, 515–527.

Bennett M, Onnebo S, Azevedo C, Saiardi A (2006). Inositol pyrophosphates: metabolism and signaling. Cell Mol Life Sci 63, 552–564.

Berchtold D, Piccolis M, Chiaruttini N, Riezman I, Riezman H, Roux A, Walther TC, Loewith R (2012). Plasma membrane stress induces relocalization of Slm proteins and activation of TORC2 to promote sphingolipid synthesis. Nat Cell Biol 14, 542–547.

Bishop AC, Ubersax JA, Petsch DT, Matheos DP, Gray NS, Blethrow J, Shimizu E, Tsien JZ, Schultz PG, Rose MD, *et al.* (2000). A chemical switch for inhibitor-sensitive alleles of any protein kinase. Nature 407, 395–401.

Bodenmiller B, Wanka S, Kraft C, Urban J, Campbell D, Pedrioli PG, Gerrits B, Picotti P, Lam H, Vitek O, *et al.* (2010). Phosphoproteomic analysis reveals interconnected system-wide responses to perturbations of kinases and phosphatases in yeast. Sci Signal 3, rs4–rs4.

Boumann HA, Chin PT, Heck AJ, De Kruijff B, De Kroon AI (2004a). The yeast phospholipid N-methyltransferases catalyzing the synthesis of phosphatidylcholine preferentially convert di-C16:1 substrates both in vivo and in vitro. J Biol Chem 279, 40314–40319.

Boumann HA, Damen MJ, Versluis C, Heck AJ, de Kruijff B, de Kroon AI (2003). The two biosynthetic routes leading to phosphatidylcholine in yeast produce different sets of molecular species. Evidence for lipid remodeling. Biochemistry 42, 3054–3059.

Boumann HA, de Kruijff B, Heck AJ, de Kroon AI (2004b). The selective utilization of substrates in vivo by the phosphatidylethanolamine and phosphatidylcholine biosynthetic enzymes Ept1p and Cpt1p in yeast. FEBS Lett 569, 173–177.

Bowdish KS, Yuan HE, Mitchell AP (1994). Analysis of RIM11, a yeast protein kinase that phosphorylates the meiotic activator IME1. Mol Cell Biol 14, 7909–7919.

Breitkreutz A, Choi H, Sharom JR, Boucher L, Neduva V, Larsen B, Lin ZY, Breitkreutz BJ, Stark C, Liu G, *et al.* (2010). A global protein kinase and phosphatase interaction network in yeast. Science 328, 1043–1046.

Breslow DK, Weissman JS (2010). Membranes in balance: mechanisms of sphingolipid homeostasis. Mol Cell 40, 267–279.

Brice SE, Alford CW, Cowart LA (2009). Modulation of sphingolipid metabolism by the phosphatidylinositol-4-phosphate phosphatase Sac1p through regulation of phosphatidylinositol in Saccharomyces cerevisiae. J Biol Chem 284, 7588–7596.

Brown HA, Murphy RC (2009). Working towards an exegesis for lipids in biology. Nat Chem Biol 5, 602–606.

Carman GM, Han G-S (2011). Regulation of phospholipid synthesis in the yeast Saccharomyces cerevisiae. Annu Rev Biochem 80, 859–883.

Carman GM, Henry SA (1999). Phospholipid biosynthesis in the yeast Saccharomyces cerevisiae and interrelationship with other metabolic processes. Prog Lipid Res 38, 361–399.
Carman GM, Kersting MC (2004). Phospholipid synthesis in yeast: regulation by phosphorylation. Biochem Cell Biol 82, 62–70.
Celenza JL, Carlson M (1984). Structure and expression of the SNF1 gene of Saccharomyces cerevisiae. Mol Cell Biol 4, 54–60.
Cheng J, Park TS, Fischl AS, Ye XS (2001). Cell cycle progression and cell polarity require sphingolipid biosynthesis in Aspergillus nidulans. Mol Cell Biol 21, 6198–6209.
Choi HS, Han GS, Carman GM (2010). Phosphorylation of yeast phosphatidylserine synthase by protein kinase A: identification of SER46 and SER47 as major sites of phosphorylation. J Biol Chem 285, 11526–11536.
Cookson MR, Lee YJ, Wang S, Slone SR, Yacoubian TA, Witt SN (2011). Defects in very long chain fatty acid synthesis enhance alpha-synuclein toxicity in a yeast model of Parkinson's disease. PLoS One 6, e15946.
Cowart LA, Hannun YA (2007). Selective substrate supply in the regulation of yeast de novo sphingolipid synthesis. J Biol Chem 282, 12330–12340.
Daum G, Lees ND, Bard M, Dickson R (1998). Biochemistry, cell biology and molecular biology of lipids of Saccharomyces cerevisiae. Yeast 14, 1471–1510.
de Kroon AIPM (2007). Metabolism of phosphatidylcholine and its implications for lipid acyl chain composition in Saccharomyces cerevisiae. Biochim Biophys Acta 1771, 343–352.
Dennis EA, Deems RA, Harkewicz R, Quehenberger O, Brown HA, Milne SB, Myers DS, Glass CK, Hardiman G, Reichart D, *et al.* (2010). A mouse macrophage lipidome. J Biol Chem 285, 39976–39985.
De Smet CH, Vittone E, Scherer M, Houweling M, Liebisch G, Brouwers JF, de Kroon AIPM (2012). The yeast acyltransferase Sct1p regulates fatty acid desaturation by competing with the desaturase Ole1p. Mol Biol Cell 23, 1146–115.
Dickson RC (2008). Thematic review series: sphingolipids. New insights into sphingolipid metabolism and function in budding yeast. J Lipid Res 49, 909–921.
Dowhan W (1997). Molecular basis for membrane phospholipid diversity: why are there so many lipids? Annu Rev Biochem 66, 199–232.
Ejsing CS, Sampaio JL, Surendranath V, Duchoslav E, Ekroos K, Klemm RW, Simons K, Shevchenko A (2009). Global analysis of the yeast lipidome by quantitative shotgun mass spectrometry. Proc Natl Acad Sci USA 106, 2136–2141.
Fiedler D, Braberg H, Mehta M, Chechik G, Cagney G, Mukherjee P, Silva AC, Shales M, Collins SR, van Wageningen S, *et al.* (2009). Functional organization of the S. cerevisiae phosphorylation network. Cell 136, 952–963.
Fu S, Yang L, Li P, Hofmann O, Dicker L, Hide W, Lin X, Watkins SM, Ivanov AR, Hotamisligil GS (2011). Aberrant lipid metabolism disrupts calcium homeostasis causing liver endoplasmic reticulum stress in obesity. Nature 473, 528–531.
Gaspar ML (2006). Inositol induces a profound alteration in the pattern and rate of synthesis and turnover of membrane lipids in Saccharomyces cerevisiae. J Biol Chem 281, 22773–22785.
Gaspar ML, Hofbauer HF, Kohlwein SD, Henry SA (2011). Coordination of storage lipid synthesis and membrane biogenesis: evidence for cross-talk between triacylglycerol metabolism and phosphatidylinositol synthesis. J Biol Chem 286, 1696–1708.
Gu Z, Steinmetz LM, Gu X, Scharfe C, Davis RW, Li WH (2003). Role of duplicate genes in genetic robustness against null mutations. Nature 421, 63–66.
Guan XL, Souza CM, Pichler H, Dewhurst G, Schaad O, Kajiwara K, Wakabayashi H, Ivanova T, Castillon GA, Piccolis M, *et al.* (2009). Functional interactions between sphingolipids and sterols in biological membranes regulating cell physiology. Mol Biol Cell 20, 2083–2095.
Guan XL, Riezman I, Wenk MR, Riezman H (2010). Yeast lipid analysis and quantification by mass spectrometry. Methods Enzymol 470, 369–391.
Gulati S, Liu Y, Munkacsi AB, Wilcox L, Sturley SL (2010). Sterols and sphingolipids: dynamic duo or partners in crime. Prog Lipid Res 49, 353–365.
Hampsey M, Kinzy TG (2007). Synchronicity: policing multiple aspects of gene expression by Ctk1. Genes Dev 21, 1288–1291.
Hannich JT, Umebayashi K, Riezman H (2011). Distribution and functions of sterols and sphingolipids. Cold Spring Harb Perspect Biol 3, a004762.
Hedbacker K, Carlson M (2008). SNF1/AMPK pathways in yeast. Front Biosci 13, 2408–2420.
Henry SA, Kohlwein SD, Carman GM (2012). Metabolism and regulation of glycerolipids in the yeast Saccharomyces cerevisiae. Genetics 190, 317–349.
Hillenmeyer ME, Fung E, Wildenhain J, Pierce SE, Hoon S, Lee W, Proctor M, St Onge RP, Tyers M, Koller D, *et al.* (2008). The chemical genomic portrait of yeast: uncovering a phenotype for all genes. Science 320, 362–365.
Hirata Y, Andoh T, Asahara T, Kikuchi A (2003). Yeast glycogen synthase kinase-3 activates Msn2p-dependent transcription of stress responsive genes. Mol Biol Cell 14, 302–312.
Hohmann S (2002). Osmotic stress signaling and osmoadaptation in yeasts. Microbiol Mol Biol Rev 66, 300–372.
Holland WL, Summers SA (2008). Sphingolipids, insulin resistance, and metabolic disease: new insights from in vivo manipulation of sphingolipid metabolism. Endocr Rev 29, 381–402.
Huang D, Moffat J, Andrews B (2002). Dissection of a complex phenotype by functional genomics reveals roles for the yeast cyclin-dependent protein kinase Pho85 in stress adaptation and cell integrity. Mol Cell Biol 22, 5076–5088.
Jesch SA, Gaspar ML, Stefan CJ, Aregullin MA, Henry SA (2010). Interruption of Inositol sphingolipid synthesis triggers Stt4p-dependent protein kinase C signaling. J Biol Chem 285, 41947–41960.
Jewett MC, Workman CT, Nookaew I, Pizarro FA, Agosin E, Hellgren LI, Nielsen J (2013). Mapping condition-dependent regulation of lipid metabolism in Saccharomyces cerevisiae. G3 (Bethesda) 3, 1979–1995.
Kaur P, Rizk N, Ibrahim S, Luo Y, Younes N, Perry B, Dennis K, Zirie M, Luta G, Cheema AK (2013). Quantitative metabolomic and lipidomic profiling reveals aberrant amino acid metabolism in type 2 diabetes. Mol BioSystems 9, 307–317.
Kim J, Kim Young C, Fang C, Russell Ryan C, Kim Jeong H, Fan W, Liu R, Zhong Q, Guan K-L (2013). Differential regulation of distinct Vps34 complexes by AMPK in nutrient stress and autophagy. Cell 152, 290–303.
Klose C, Surma MA, Gerl MJ, Meyenhofer F, Shevchenko A, Simons K (2012). Flexibility of a eukaryotic lipidome—insights from yeast lipidomics. PLoS One 7, e35063.
Kobayashi SD, Nagiec MM (2003). Ceramide/long-chain base phosphate rheostat in Saccharomyces cerevisiae: regulation of ceramide synthesis by Elo3p and Cka2p. Eukaryot Cell 2, 284–294.
Lee YS, Mulugu S, York JD, O'Shea EK (2007). Regulation of a cyclin-CDK-CDK inhibitor complex by inositol pyrophosphates. Science 316, 109–112.
Leonard TA, Hurley JH (2011). Regulation of protein kinases by lipids. Curr Opin Struct Biol 21, 785–791.
Li J, Yuan Z, Zhang Z (2010). The cellular robustness by genetic redundancy in budding yeast. PLoS Genet 6, e1001187.
Liu M, Huang C, Polu SR, Schneiter R, Chang A (2012). Regulation of sphingolipid synthesis through Orm1 and Orm2 in yeast. J Cell Sci 125, 2428–2435.
Livak KJ, Schmittgen TD (2001). Analysis of relative gene expression data using real-time quantitative PCR and the 2–ΔΔCT method. Methods 25, 402–408.
Lykidis A (2007). Comparative genomics and evolution of eukaryotic phospholipid biosynthesis. Prog Lipid Res 46, 171–199.
Manning G, Plowman GD, Hunter T, Sudarsanam S (2002). Evolution of protein kinase signaling from yeast to man. Trends Biochem Sci 27, 514–520.
Momcilovic M, Carlson M (2011). Alterations at dispersed sites cause phosphorylation and activation of SNF1 protein kinase during growth on high glucose. J Biol Chem 286, 23544–23551.
Munn AL, Heese-Peck A, Stevenson BJ, Pichler H, Riezman H (1999). Specific sterols required for the internalization step of endocytosis in yeast. Mol Biol Cell 10, 3943–3957.
Muthusamy BP, Raychaudhuri S, Natarajan P, Abe F, Liu K, Prinz WA, Graham TR (2009). Control of protein and sterol trafficking by antagonistic activities of a type IV P-type ATPase and oxysterol binding protein homologue. Mol Biol Cell 20, 2920–2931.
Nakano K, Yamamoto T, Kishimoto T, Noji T, Tanaka K (2008). Protein kinases Fpk1p and Fpk2p are novel regulators of phospholipid asymmetry. Mol Biol Cell 19, 1783–1797.
Nielsen J (2009). Systems biology of lipid metabolism: from yeast to human. FEBS Lett 583, 3905–3913.
Nohturfft A, Zhang SC (2009). Coordination of lipid metabolism in membrane biogenesis. Annu Rev Cell Dev Biol 25, 539–566.
Obara K, Noda T, Niimi K, Ohsumi Y (2008). Transport of phosphatidylinositol 3-phosphate into the vacuole via autophagic membranes in Saccharomyces cerevisiae. Genes Cells 13, 537–547.

O'Neill EM, Kaffman A, Jolly ER, O'Shea EK (1996). Regulation of PHO4 nuclear localization by the PHO80-PHO85 cyclin-CDK complex. Science 271, 209–212.
Outeiro TF, Muchowski PJ (2004). Molecular genetics approaches in yeast to study amyloid diseases. J Mol Neurosci 23, 49–60.
Petranovic D, Tyo K, Vemuri GN, Nielsen J (2010). Prospects of yeast systems biology for human health: integrating lipid, protein and energy metabolism. FEMS Yeast Res 10, 1046–1059.
Polge C, Thomas M (2007). SNF1/AMPK/SnRK1 kinases, global regulators at the heart of energy control? Trends Plant Sci 12, 20–28.
Ptacek J, Devgan G, Michaud G, Zhu H, Zhu X, Fasolo J, Guo H, Jona G, Breitkreutz A, Sopko R, *et al*. (2005). Global analysis of protein phosphorylation in yeast. Nature 438, 679–684.
Rajakumari S, Rajasekharan R, Daum G (2010). Triacylglycerol lipolysis is linked to sphingolipid and phospholipid metabolism of the yeast Saccharomyces cerevisiae. Biochim Biophys Acta 1801, 1314–1322.
Rapold RA, Wueest S, Knoepfel A, Schoenle EJ, Konrad D (2013). Fas activates lipolysis in a Ca2+-CaMKII-dependent manner in 3T3-L1 adipocytes. J Lipid Res 54, 63–70.
Roelants FM, Baltz AG, Trott AE, Fereres S, Thorner J (2009). A protein kinase network regulates the function of aminophospholipid flippases. Proc Natl Acad Sci USA 107, 34–39.
Roelants FM, Baltz AG, Trott AE, Fereres S, Thorner J (2010). A protein kinase network regulates the function of aminophospholipid flippases. Proc Natl Acad Sci USA 107, 34–39.
Roelants FM, Breslow DK, Muir A, Weissman JS, Thorner J (2011). Protein kinase Ypk1 phosphorylates regulatory proteins Orm1 and Orm2 to control sphingolipid homeostasis in Saccharomyces cerevisiae. Proc Natl Acad Sci USA 108, 19222–19227.
Sampaio JL, Gerl MJ, Klose C, Ejsing CS, Beug H, Simons K, Shevchenko A (2011). Membrane lipidome of an epithelial cell line. Proc Natl Acad Sci USA 108, 1903–1907.
Santos AX, Riezman H (2012). Yeast as a model system for studying lipid homeostasis and function. FEBS Lett 586, 2858–2867.
Schneiter R, Brugger B, Amann CM, Prestwich GD, Epand RF, Zellnig G, Wieland FT, Epand RM (2004). Identification and biophysical characterization of a very-long-chain-fatty-acid-substituted phosphatidylinositol in yeast subcellular membranes. Biochem J 381, 941–949.
Schuiki I, Schnabl M, Czabany T, Hrastnik C, Daum G (2010). Phosphatidylethanolamine synthesized by four different pathways is supplied to the plasma membrane of the yeast Saccharomyces cerevisiae. Biochim Biophys Acta 1801, 480–486.
Sharifpoor S, van Dyk D, Costanzo M, Baryshnikova A, Friesen H, Douglas AC, Youn J-Y, VanderSluis B, Myers CL, Papp B, *et al*. (2012). Functional wiring of the yeast kinome revealed by global analysis of genetic network motifs. Genome Res 22, 791–801.
Shimobayashi M, Oppliger W, Moes S, Jenö P, Hall MN (2013). TORC1-regulated protein kinase Npr1 phosphorylates Orm to stimulate complex sphingolipid synthesis. Mol Biol Cell 24, 870–881.
Shin GH, Veen M, Stahl U, Lang C (2012). Overexpression of genes of the fatty acid biosynthetic pathway leads to accumulation of sterols in Saccharomyces cerevisiae. Yeast 29, 371–383.
Shirra MK, Patton-Vogt J, Ulrich A, Liuta-Tehlivets O, Kohlwein SD, Henry SA, Arndt KM (2001). Inhibition of acetyl coenzyme A carboxylase activity restores expression of the INO1 gene in a snf1 mutant strain of Saccharomyces cerevisiae. Mol Cell Biol 21, 5710–5722.
Smolenska-Sym G, Spychalska J, Zdebska E, Wozniak J, Traczyk Z, Pszenna E, Maj S, Danikiewicz W, Bienkowski T, Koscielak J (2004). Ceramides and glycosphingolipids in maturation process: leukemic cells as an experimental model. Blood Cells Mol Dis 33, 68–76.
Strahl T, Thorner J (2007). Synthesis and function of membrane phosphoinositides in budding yeast, Saccharomyces cerevisiae. Biochim Biophys Acta 1771, 353–404.
Stukey JE, McDonough VM, Martin CE (1989). Isolation and characterization of OLE1, a gene affecting fatty acid desaturation from Saccharomyces cerevisiae. J Biol Chem 264, 16537–16544.
Sturley SL (2000). Conservation of eukaryotic sterol homeostasis: new insights from studies in budding yeast. Biochim Biophys Acta 1529, 155–163.
Summers SA (2010). Sphingolipids and insulin resistance: the five Ws. Curr Opin Lipidol 21, 128–135.
Sun Y, Miao Y, Yamane Y, Zhang C, Shokat KM, Takematsu H, Kozutsumi Y, Drubin DG (2012). Orm protein phosphoregulation mediates transient sphingolipid biosynthesis response to heat stress via the Pkh-Ypk and Cdc55-PP2A pathways. Mol Biol Cell 23, 2388–2398.
Surma Michal A, Klose C, Peng D, Shales M, Mrejen C, Stefanko A, Braberg H, Gordon David E, Vorkel D, Ejsing Christer S, *et al*. (2013). A lipid E-MAP identifies Ubx2 as a critical regulator of lipid saturation and lipid bilayer stress. Mol Cell 51, 519–530.
Tan CS (2011). Sequence, structure, and network evolution of protein phosphorylation. Sci Signal 4, mr6.
Tan CSH, Bodenmiller B, Pasculescu A, Jovanovic M, Hengartner MO, Jorgensen C, Bader GD, Aebersold R, Pawson T, Linding R (2009). Comparative analysis reveals conserved protein phosphorylation networks implicated in multiple diseases. Sci Signal 2, ra39–ra39.
Tanigawa M, Kihara A, Terashima M, Takahara T, Maeda T (2012). Sphingolipids regulate the yeast high-osmolarity glycerol response pathway. Mol Cell Biol 32, 2861–2870.
Tarasov K, Stefanko A, Casanovas A, Surma M, Berzina Z, Hannibal-Bach HK, Ekroos K, Ejsing C (2014). High-content screening of yeast mutant libraries by shotgun lipidomics. Mol BioSystems 10, 1364–1376.
Tavassoli S, Chao JT, Young BP, Cox RC, Prinz WA, de Kroon AI, Loewen CJ (2013). Plasma membrane-endoplasmic reticulum contact sites regulate phosphatidylcholine synthesis. EMBO Rep 14, 434–440.
Tehlivets O, Scheuringer K, Kohlwein SD (2007). Fatty acid synthesis and elongation in yeast. Biochim Biophys Acta 1771, 255–270.
Tuller G, Nemec T, Hrastnik C, Daum G (1999). Lipid composition of subcellular membranes of an FY1679-derived haploid yeast wild-type strain grown on different carbon sources. Yeast 15, 1555–1564.
Umebayashi K, Nakano A (2003). Ergosterol is required for targeting of tryptophan permease to the yeast plasma membrane. J Cell Biol 161, 1117–1131.
Usaite R, Jewett MC, Oliveira AP, Yates JR, Olsson L, Nielsen J (2009). Reconstruction of the yeast Snf1 kinase regulatory network reveals its role as a global energy regulator. Mol Systems Biol 5, 319.
Vionnet C, Roubaty C, Ejsing CS, Knudsen J, Conzelmann A (2010). Yeast cells lacking all known ceramide synthases continue to make complex sphingolipids and to incorporate ceramides into glycosylphosphatidylinositol (GPI) anchors. J Biol Chem 286, 6769–6779.
Wagner A (2002). Asymmetric functional divergence of duplicate genes in yeast. Mol Biol Evolut 19, 1760–1768.
Woods A, Munday MR, Scott J, Yang X, Carlson M, Carling D (1994). Yeast SNF1 is functionally related to mammalian AMP-activated protein kinase and regulates acetyl-CoA carboxylase in vivo. J Biol Chem 269, 19509–19515.
Young BP, Shin JJH, Orij R, Chao JT, Li SC, Guan XL, Khong A, Jan E, Wenk MR, Prinz WA, *et al*. (2010). Phosphatidic acid is a pH biosensor that links membrane biogenesis to metabolism. Science 329, 1085–1088.
Zaman S, Lippman SI, Zhao X, Broach JR (2008). How Saccharomyces responds to nutrients. Annu Rev Genet 42, 27–81.
Zhang J, Vaga S, Chumnanpuen P, Kumar R, Vemuri GN, Aebersold R, Nielsen J (2011). Mapping the interaction of Snf1 with TORC1 in Saccharomyces cerevisiae. Mol Syst Biol 7, 545.
Zhang L, Díaz–Díaz N, Zarringhalam K, Hermansson M, Somerharju P, Chuang J (2012). Dynamics of the ethanolamine glycerophospholipid remodeling network. PLoS One 7, e50858.
Zhang XD (2007). A new method with flexible and balanced control of false negatives and false positives for hit selection in RNA interference high-throughput screening assays. J Biomol Screen 12, 645–655.
Zhang XD, Ferrer M, Espeseth AS, Marine SD, Stec EM, Crackower MA, Holder DJ, Heyse JF, Strulovici B (2007). the use of strictly standardized mean difference for hit selection in primary RNA interference high-throughput screening experiments. J Biomol Screen 12, 497–509.
Zhou X, O'Shea E K (2011). Integrated approaches reveal determinants of genome-wide binding and function of the transcription factor Pho4. Mol Cell 42, 826–836.
Zinser E, Paltauf F, Daum G (1993). Sterol composition of yeast organelle membranes and subcellular distribution of enzymes involved in sterol metabolism. J Bacteriol 175, 2853–2858.